

The nucleon axial charge in lattice QCD with controlled errors

S. Capitani,^{1,2} M. Della Morte,^{1,2} G. von Hippel,¹ B. Jäger,^{1,2}
A. Jüttner,³ B. Knippschild,¹ H.B. Meyer,¹ and H. Wittig^{1,2,*}

¹*Institut für Kernphysik, University of Mainz, Becher Weg 45, D-55099 Mainz, Germany*

²*Helmholtz Institute Mainz, University of Mainz, D-55099 Mainz, Germany*

³*CERN, Physics Department, Theory Division, CH-1211 Geneva 23, Switzerland*

(Dated: September 2012)

We report on our calculation of the nucleon axial charge g_A in QCD with two flavours of dynamical quarks. A detailed investigation of systematic errors is performed, with a particular focus on contributions from excited states to three-point correlation functions. The use of summed operator insertions allows for a much better control over such contamination. After performing a chiral extrapolation to the physical pion mass, we find $g_A = 1.223 \pm 0.063$ (stat) $_{-0.060}^{+0.035}$ (syst), in good agreement with the experimental value.

I. INTRODUCTION

Lattice simulations of Quantum Chromodynamics (QCD) have, by now, reached a stage which allows for first-principles determinations of many hadronic properties, with overall uncertainties at the percent level [1]. While systematic errors for quantities such as quark masses, meson decay constants and form factors appear very well controlled, the situation regarding properties of the nucleon is less satisfactory. For instance, lattice calculations have so far failed in reproducing the well-known experimental findings on nucleon structure (see [2, 3] for recent reviews). A prominent example is the axial charge, g_A , of the nucleon. Lattice results for this quantity lie typically 10 – 15% below the experimental value [4–16]. What is even more worrying is the absence of any tendency in the lattice data which would indicate that the gap is narrowing as the pion mass is decreased — in fact, the opposite trend is often observed. The most likely explanation is that systematic effects are not fully controlled. What is lacking, therefore, is a benchmark calculation of a quantity which describes basic structural properties of the nucleon, and for this purpose the axial charge is an ideal candidate: (1) it is derived from a matrix element of a simple fermionic bilinear which contains no derivatives, (2) the initial and final states can both be considered at rest, and (3) its definition as an isovector quantity implies that contributions from quark-disconnected diagrams are absent.

In this paper, we report on our results for g_A addressing in detail all sources of systematic errors, such as lattice artefacts, finite-volume effects, and chiral extrapolations. We specifically focus on the problem of a systematic bias arising from excited state contributions in the relevant correlation functions. To this end, we apply the method of summed operator insertions, which helps to control any such contamination.

II. SIMULATION DETAILS

Our simulations are performed with $N_f = 2$ flavours of $O(a)$ improved Wilson fermions and the Wilson plaquette action. We stress that excited state contamination is an important issue for lattice simulations with any number of dynamical quarks. Hence, the question whether estimates for g_A may be biased can be adequately addressed in two-flavour QCD. In particular, there is ample evidence [1] that there are no discernible differences between QCD with $N_f = 2$ and $N_f = 2 + 1$ flavours at the few-percent level. Therefore, the observed gap between previous lattice estimates of the axial charge and its experimental value is by far too large to be explained by the presence or absence of a dynamical strange quark.

We use the non-perturbative determination of the improvement coefficient c_{sw} from ref. [17]. Table I contains a compilation of lattice sizes and other simulation parameters, including the pion and nucleon masses in lattice units. All listed ensembles were generated as part of the CLS initiative, employing the deflation-accelerated DD-HMC algorithm [18, 19]. Quark propagators were computed using Gaussian-smearing source vectors [20] supplemented by HYP-smearing links [21]. The smearing parameters were tuned to maximize plateau lengths for effective masses for a variety of channels. On each ensemble we collected between 150 and 250 highly decorrelated configurations. Up to eight sources, equally spaced in the temporal direction, were used to reduce statistical fluctuations in correlation functions. In this way, we performed between 280 and 1700 individual measurements on our ensembles. The lattice spacings were determined using the mass of the Ω baryon as described in [22]. As we are in the process of supplementing the set of our ensembles, estimates of the lattice spacing will be updated in the future. Correlation functions were computed using the same smeared nucleon interpolating operators at the source and sink. For three-point functions we employed the improved axial current which is related to its renormalized counterpart via [23]

$$(A_\mu^R) = Z_A(1 + b_A am_q)(A_\mu + ac_A \partial_\mu P), \quad (1)$$

where A_μ and P denote the local axial current and pseu-

* Email:wittig@kph.uni-mainz.de

Run	L/a	β	κ	am_π	am_N	$m_\pi L$	N_{cfg}	N_{src}
A2	32	5.2	0.13565	0.2424(4)	0.592(4)	7.73	144	4
A3	32	5.2	0.13580	0.1893(5)	0.531(4)	6.06	265	4
A4	32	5.2	0.13590	0.1454(7)	0.481(6)	4.65	199	4
A5	32	5.2	0.13594	0.1249(14)	0.469(8)	4.00	212	8
E3	32	5.3	0.13605	0.2071(6)	0.510(3)	6.63	139	2
E4	32	5.3	0.13610	0.1934(5)	0.497(3)	6.19	162	8
E5	32	5.3	0.13625	0.1439(6)	0.420(3)	4.60	168	8
F6	48	5.3	0.13635	0.1036(5)	0.382(5)	4.97	199	4
F7	48	5.3	0.13538	0.0886(4)	0.334(8)	4.25	250	4
N4	48	5.5	0.13650	0.1358(3)	0.351(2)	6.52	150	4
N5	48	5.5	0.13660	0.1090(3)	0.320(3)	5.23	150	4

TABLE I. Simulation parameters, pion and nucleon masses for all ensembles used in this paper. The temporal extent of each lattice is twice the spatial length, $T = 2L$. N_{cfg} is the number of configurations per ensemble, while N_{src} denotes the number of different sources.

doscalar density, respectively, and m_q is the bare subtracted quark mass. Since g_A was determined from the 3rd component of the axial current alone, the contribution proportional to $\partial_\mu P$ vanishes, as the axial charge is defined at zero momentum transfer. Non-perturbative values for the renormalization factor Z_A were taken from ref. [24], while the improvement coefficient b_A was estimated in tadpole-improved perturbation theory [25]. Since the contribution from the improvement term is at the sub-percent level in the range of quark masses considered, the systematic effect arising from the unknown non-perturbative value for b_A will be negligible.

III. EXCITED STATE CONTAMINATION

We denote the Euclidean time separation between the nucleon source and sink by t_s , while t with $t \leq t_s$ marks the interval between the source and the axial current. If, as in our case, the same smeared interpolating operators are applied at the source and sink, the axial charge can be determined from a simple ratio,

$$R(t, t_s) := \frac{C_3^A(t, t_s)}{C_2(t_s)}, \quad (2)$$

where $C_3^A(t, t_s)$ denotes the three-point correlation function of the local, bare axial current at vanishing momentum transfer. For large values of t and t_s the ratio $R(t, t_s)$ yields directly the bare axial charge, i.e.

$$R(t, t_s) \xrightarrow{t, (t_s-t) \gg 0} g_A^{\text{bare}} + \mathcal{O}(e^{-\Delta t}) + \mathcal{O}(e^{-\Delta(t_s-t)}), \quad (3)$$

where Δ denotes the gap between the masses of the nucleon and its first excitation. The axial charge is usually extracted by fitting $R(t, t_s)$ to a constant. Due to the exponentially increasing noise-to-signal ratio in correlation functions of the nucleon, typical values of t_s are of the

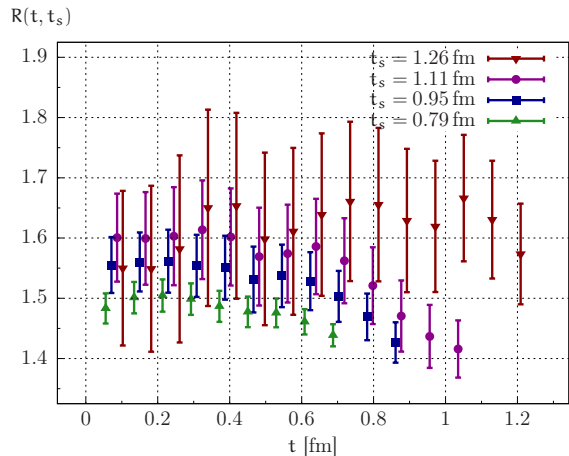


FIG. 1. The ratio $R(t, t_s)$ at $\beta = 5.2$ and $m_\pi = 312$ MeV for several different values of the source-sink separation t_s .

order of 1 fm. To guarantee a reliable determination of g_A , excited state contributions in eq. (3) must already be sufficiently suppressed for $t, (t_s - t) \lesssim 0.5$ fm.

The lowest-lying multi-particle state in the nucleon channel consists of one nucleon and two pions forming an S-wave. Therefore, assuming that nucleon and pions are only weakly interacting, one expects the gap Δ to be proportional to the pion mass, since the mass difference to the Roper resonance amounts to about 500 MeV. The same argument applies if one nucleon and one pion form a P-wave, provided that the non-zero momentum induced by the box size is small enough. It is then clear that excited states may increasingly distort the results for g_A as the physical pion mass is approached. A typical situation is shown in Fig. 1: as t_s is varied from 0.8 fm to 1.26 fm, the ratio $R(t, t_s)$ is shifted by about 10% to larger values. Given the rapid degradation of the signal, it then remains unclear whether $t_s \approx 1$ fm is sufficient to rule out a bias in the result for g_A . The most straightforward strategy to address this problem is to include the first excitation into the fit *ansatz* for $R(t, t_s)$ (see ref. [26]) or to investigate larger values of t and t_s [27].

Here we present an alternative approach, based on the use of summed operator insertions [20, 28, 29]. The key observation is that excited state contributions can be parametrically reduced when $R(t, t_s)$ is summed over t . More precisely, the asymptotic behaviour of the summed ratio $S(t_s)$ is given by

$$S(t_s) := \sum_{t=0}^{t_s} R(t, t_s) \xrightarrow{t_s \gg 0} c + t_s \{g_A^{\text{bare}} + \mathcal{O}(e^{-\Delta t_s})\}, \quad (4)$$

where the (divergent) constant, c , includes contributions from contact terms. By computing $S(t_s)$ for several sufficiently large values of t_s , the quantity of interest can be extracted from the slope of a linear fit. Since $t_s > t, (t_s - t)$ by construction, excited state contributions to the slope of $S(t_s)$ are more strongly suppressed

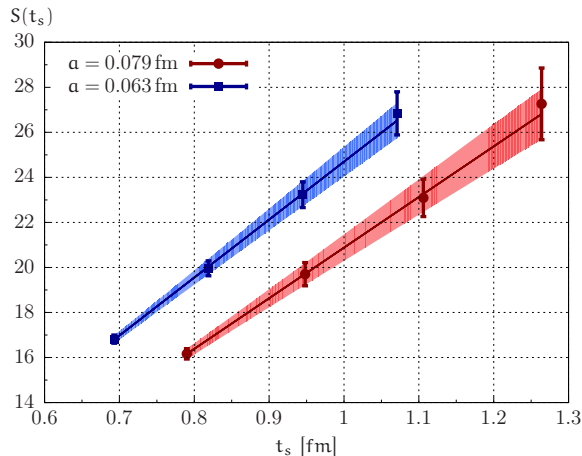


FIG. 2. The summed ratio $S(t_s)$ at $m_\pi \approx 320$ MeV for two different lattice spacings (ensembles A5 and F6).

relative to $R(t, t_s)$. Compared to the standard method of computing the latter at a single fixed value of t_s , it is clear, however, that the approach via summed insertions is computationally more demanding. In Fig. 2 we show typical fits to the summed ratio $S(t_s)$ which demonstrate that the linear behaviour is very well satisfied.

IV. RESULTS

We have determined the axial charge by fitting the summed correlator $S(t_s)$ to a linear function for $0.7 \text{ fm} \lesssim t_s \lesssim 1.3 \text{ fm}$ and multiplying the slope by the relevant renormalization factor of the axial current, eq. (1). We have verified the stability of the method by excluding the smallest value of t_s from the fit for each ensemble. Typically, this leads to an increase in the value for g_A , albeit with a 1.5 – 2 times larger statistical error.

In the following we present a detailed comparison between the results obtained using summed insertions (“summation method”) with those arising from fitting the ratio $R(t, t_s)$ to a constant in t for $t_s \approx 1.1 \text{ fm}$ (“plateau method”). Results are shown in Table II and Fig. 3. One observes that the plateau method yields estimates for g_A that mostly lie below the experimental value, which is the typical behaviour seen in other calculations at similar pion masses. Typically, the summation method produces results which are higher than those from the plateau method, in some cases by up to 10%. At the same time, the summation method has larger statistical errors. Still, since an increase is observed in seven out of eleven cases, while a slightly smaller value was obtained only for one ensemble, it is unlikely that this can be merely attributed to statistical fluctuations.

In order to investigate the chiral behaviour in detail, we have performed chiral extrapolations based on several different *ansätze* commonly used in the literature [7, 8, 13,

Run	a [fm]	m_π [MeV]	m_N/m_π	g_A^{summ}	g_A^{plat}
A2	0.079	603	2.454(15)	1.179(45)	1.195(28)
A3		473	2.803(23)	1.256(52)	1.256(28)
A4		363	3.309(41)	1.084(103)	1.121(42)
A5		312	3.751(77)	1.382(127)	1.228(61)
E3	0.063	649	2.462(12)	1.212(49)	1.195(40)
E4		606	2.561(11)	1.154(68)	1.160(36)
E5		451	2.920(22)	1.311(105)	1.184(52)
F6		324	3.683(48)	1.268(91)	1.217(55)
F7		277	3.771(86)	1.162(95)	1.137(37)
N4	0.050	536	2.581(13)	1.221(32)	1.176(26)
N5		430	2.939(28)	1.212(48)	1.180(37)

TABLE II. Results for the axial charge determined via summed insertions and the conventional plateau method. The data are corrected for finite-volume effects estimated in HBChPT (see text).

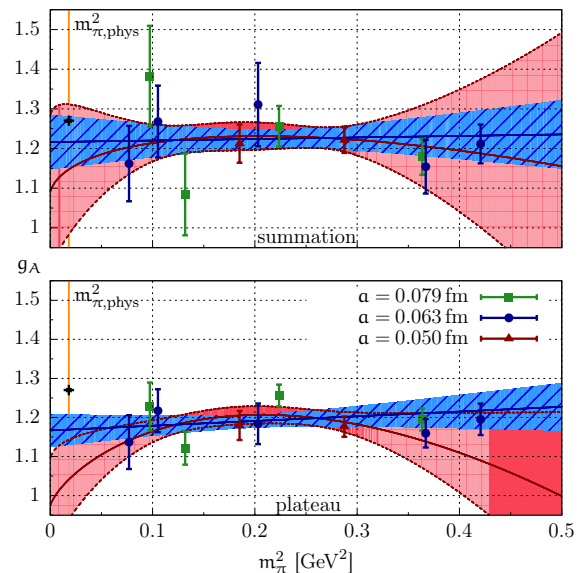


FIG. 3. Chiral behaviour of g_A extracted from summed insertions (upper panel) and using the standard plateau method (lower panel). Chiral fits of type “A” and “D” (see text) applied for $m_\pi < 540$ MeV are represented by the blue/hatched and red bands, respectively. The black point denotes the experimental value.

14, 30], i.e.

$$\begin{aligned}
 \text{Fit A: } & \alpha + \beta m_\pi^2 \\
 \text{Fit B: } & \alpha' + \beta' m_\pi^2 - |\gamma'| m_\pi^2 \ln m_\pi^2 / \Lambda^2 \\
 \text{Fit C: } & \alpha'' + \beta'' m_\pi^2 - |\gamma''| e^{-m_\pi L},
 \end{aligned} \tag{5}$$

with fit parameters $\alpha, \beta, \alpha', \dots$. Another *ansatz*, Fit D, is a three-parameter fit, based on the expressions derived in Heavy-Baryon Chiral Perturbation Theory (HBChPT) in infinite volume [31, 32], with three additional low-energy constants fixed by phenomenology [14]. Examples are

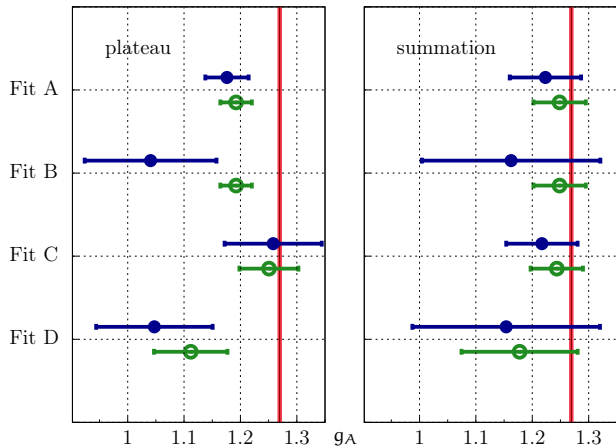


FIG. 4. Results for g_A at the physical pion mass for the plateau and summation methods. Solid points refer to a pion mass cut at $m_\pi < 540$ MeV, while open symbols are used to denote results from fits across the entire pion mass range. Fits A, B and D were applied to the volume-corrected data (see text). The vertical lines represent the experimental value.

shown in Fig. 3. A simple linear chiral extrapolation (Fit A) applied to the data from all three lattice spacings for which $m_\pi < 540$ MeV yields a value for g_A at the physical pion mass which agrees well with experiment within the statistical uncertainty. A similar statement applies to the fit based on HBChPT (Fit D). By contrast, extrapolations of the data determined using the plateau method fail to reproduce the experimental value by two standard deviations.

Fit C was introduced in [8] to test whether the widely observed underestimates of g_A could be a manifestation of finite-volume effects. After determining the parameters α'' , β'' and γ'' , the volume-dependent term proportional to $\exp\{-m_\pi L\}$ can be subtracted. Indeed, a non-zero value for γ'' results when fit C is applied to the data obtained via the plateau method. A linear chiral extrapolation, using the fitted coefficients α'' and β'' , then yields an estimate for g_A which agrees with experiment (see Fig. 4). However, repeating the procedure for the summation method produces a vanishing coefficient γ'' . We conclude that, in this case, there is no need to subtract any term designed to account for finite-volume effects, in order to get agreement with experiment. When addressing the influence of excited states it is important to realize that such contributions are volume-dependent, whenever they are due to multiple-particle states. Thus, for a true benchmark calculation of the axial charge one must be able to separate finite-volume corrections to g_A from volume-dependent excited-state contamination.

Figure 4 shows a compilation of the chirally extrapolated g_A from the four different fit types. While summed insertions invariably produce estimates that are compatible with experiment, one consistently obtains lower values using the plateau method, except for fit C with the

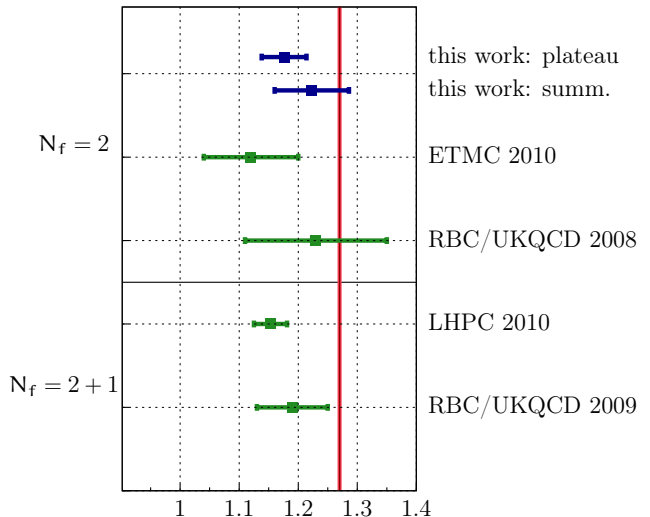


FIG. 5. Estimates for g_A determined from the summation and plateau methods compared to recent results by ETMC [14], RBC/UKQCD ([9] for $N_f = 2$, ref. [10] for $N_f = 2 + 1$) and LHPC [13]. Only statistical errors are shown. The thick vertical line represents the experimental result.

term containing $\exp\{-m_\pi L\}$ subtracted. These observations are stable under variations of the pion mass range, as indicated in the figure.

We now proceed to discussing our final result and the estimation of systematic errors. We applied a finite-volume correction based on the expression derived in HBChPT [31] (see ref. [14] for details on the numerical evaluation). Since $m_\pi L > 4$ and $2 \text{ fm} \leq L \leq 3 \text{ fm}$ the resulting shifts are at the sub-percent level for all our ensembles. As our best estimate, we quote the result from fit A, applied to the volume-corrected data obtained from summed insertions, with a cut of $m_\pi < 540$ MeV, i.e.

$$g_A = 1.223 \pm 0.063 \text{ (stat)}, \quad (6)$$

which agrees with the PDG average [33] of 1.2701(25) within the statistical error. By contrast, when the same fitting procedure is applied to the results extracted from the plateau method, one finds the much lower estimate of $g_A = 1.173 \pm 0.038 \text{ (stat)}$.

It is instructive to compare our findings to other recent results for the axial charge. A compilation is plotted in Fig. 5. With the exception of the results by RBC/UKQCD [9, 10], our estimate based on the summation method is the only one which agrees with the experimental value within statistical errors. It is also worth mentioning that, in order to achieve agreement with experiment, a large downward curvature in the data had to be separated off in refs. [9, 10], by applying the procedure of fit C.

We note that, with our current level of statistical accuracy, no significant dependence on the lattice spacing could be detected. For instance, applying fits A–D only

to the data at $\beta = 5.3$ produces a tiny variation, which is 10 times smaller than the statistical error. Therefore we refrain from quoting a separate systematic uncertainty relating to cutoff effects. In order to quantify the uncertainty associated with the chiral extrapolation, we adopted two procedures. First, by applying different cuts to the upper limit on the pion mass interval between 470 and 640 MeV, we observe a variation of ± 0.035 relative to the central value in eq. (6). Second, we considered the spread among fits A–D as a measure for the uncertainty relating to the extrapolation, which amounts to a downward shift by -0.060 . Taking the largest upward and downward variations from both methods as the error estimate, we arrive at our final result

$$g_A = 1.223 \pm 0.063 \text{ (stat)} \begin{smallmatrix} +0.035 \\ -0.060 \end{smallmatrix} \text{ (syst)}, \quad (7)$$

which agrees with the experimental result at the level of 6 – 7%.

V. CONCLUSIONS

The typical source-sink separations in baryonic three-point functions can be smaller by up to a factor two compared to those used in the mesonic sector. Even for $t_s \approx 1.3$ fm it is hard to judge whether or not a significant bias due to excited state contributions can be excluded, if the standard plateau method is employed without further checks (see Fig. 1). Summed operator insertions offer an attractive alternative, since excited state contri-

butions are parametrically more strongly suppressed relative to those encountered in conventional ratios. Our findings, summarized in Fig. 4, demonstrate that a much better agreement with the experimental value of g_A can be achieved in this way. On the downside, one must list the necessity to compute correlation functions for several source-sink separations, as well as the larger statistical errors associated with the method. However, since excited state contamination might be a generic problem for lattice calculations of structural properties of the nucleon, the larger numerical effort seems a worthwhile investment. We plan to corroborate our findings by including additional ensembles with smaller pion masses and extend our studies to other quantities, such as the vector and axial vector form factors of the nucleon. For this purpose, optimised anisotropic smearing functions for non-vanishing hadron momenta [34, 35] may prove to be a useful addition to the technique of summed insertions.

ACKNOWLEDGMENTS

Our calculations were performed on the “Wilson” HPC Cluster at the Institute for Nuclear Physics, University of Mainz. We are grateful to Dalibor Djukanovic for technical support. This work was supported by DFG (SFB 443 and SFB 1044) and the Rhineland-Palatinate Research Initiative. We are grateful to our colleagues within the CLS initiative for sharing ensembles.

-
- [1] G. Colangelo *et al.*, Eur. Phys. J. **C71**, 1695 (2011), arXiv:1011.4408.
 - [2] D.B. Renner, PoS **LAT2009**, 018 (2009), arXiv:1002.0925.
 - [3] C. Alexandrou, PoS **LATTICE2010**, 001 (2010), arXiv:1011.3660.
 - [4] LHP Collaboration, D. Dolgov *et al.*, Phys. Rev. **D66**, 034506 (2002), hep-lat/0201021.
 - [5] RBCK Collaboration, S. Ohta and K. Orginos, Nucl. Phys. Proc. Suppl. **140**, 396 (2005), hep-lat/0411008.
 - [6] LHP Collaboration, R. G. Edwards *et al.*, Phys. Rev. Lett. **96**, 052001 (2006), hep-lat/0510062.
 - [7] A.A. Khan *et al.*, Phys. Rev. **D74**, 094508 (2006), hep-lat/0603028.
 - [8] RBC/UKQCD Collaboration, T. Yamazaki *et al.*, Phys. Rev. Lett. **100**, 171602 (2008), arXiv:0801.4016.
 - [9] H.-W. Lin, T. Blum, S. Ohta, S. Sasaki, and T. Yamazaki, Phys. Rev. **D78**, 014505 (2008), arXiv:0802.0863.
 - [10] T. Yamazaki *et al.*, Phys. Rev. **D79**, 114505 (2009), arXiv:0904.2039.
 - [11] G. Engel *et al.*, PoS **LAT2009**, 135 (2009), arXiv:0910.4190.
 - [12] QCDSF/UKQCD Collaboration, M. Göckeler *et al.*, PoS **LAT2009**, 125 (2009), arXiv:0912.0167.
 - [13] LHP Collaboration, J. D. Bratt *et al.*, Phys. Rev. **D82**, 094502 (2010), arXiv:1001.3620.
 - [14] ETM Collaboration, C. Alexandrou *et al.*, Phys. Rev. **D83**, 045010 (2011), arXiv:1012.0857.
 - [15] QCDSF/UKQCD Collaboration, D. Pleiter *et al.*, PoS **LATTICE2010**, 153 (2010), arXiv:1101.2326.
 - [16] QCDSF/UKQCD Collaboration, M. Göckeler *et al.*, PoS **LATTICE2010**, 163 (2010), arXiv:1102.3407.
 - [17] ALPHA Collaboration, K. Jansen and R. Sommer, Nucl. Phys. **B530**, 185 (1998), hep-lat/9803017.
 - [18] M. Lüscher, Comput. Phys. Commun. **165**, 199 (2005), hep-lat/0409106.
 - [19] M. Lüscher, JHEP **12**, 011 (2007), arXiv:0710.5417.
 - [20] S. Güsken *et al.*, Phys. Lett. **B227**, 266 (1989).
 - [21] A. Hasenfratz and F. Knechtli, Phys. Rev. **D64**, 034504 (2001), hep-lat/0103029.
 - [22] S. Capitani, M. Della Morte, G. von Hippel, B. Knippschild, and H. Wittig, PoS **LATTICE2011**, 145 (2011), arXiv:1110.6365.
 - [23] M. Lüscher, S. Sint, R. Sommer, and P. Weisz, Nucl. Phys. **B478**, 365 (1996), hep-lat/9605038.
 - [24] M. Della Morte, R. Sommer, and S. Takeda, Phys. Lett. **B672**, 407 (2009), arXiv:0807.1120.
 - [25] S. Sint and P. Weisz, Nucl. Phys. **B502**, 251 (1997), hep-lat/9704001.
 - [26] J. Green, S. Krieg, J. Negele, A. Pochinsky, and S. Syritsyn, PoS **LATTICE2011**, 157 (2011), arXiv:1111.0255.
 - [27] S. Dinter *et al.*, Phys. Lett. **B704**, 89 (2011), arXiv:1108.1076.

- [28] L. Maiani, G. Martinelli, M. L. Paciello, and B. Taglienti, Nucl. Phys. **B293**, 420 (1987).
- [29] J. Bulava, M. Donnellan, and R. Sommer, JHEP **1201**, 140 (2012), arXiv:1108.3774.
- [30] G. Colangelo, A. Führer, and S. Lanz, Phys. Rev. **D82**, 034506 (2010), arXiv:1005.1485.
- [31] T.R. Hemmert, M. Procura, and W. Weise, Phys. Rev. **D68**, 075009 (2003), hep-lat/0303002.
- [32] S. R. Beane and M. J. Savage, Phys. Rev. **D70**, 074029 (2004), hep-ph/0404131.
- [33] Particle Data Group, K. Nakamura *et al.*, J. Phys. **G37**, 075021 (2010).
- [34] D.S. Roberts, W. Kamleh, D.B. Leinweber, M.S. Mahbub and B.J. Menadue, arXiv:1206.5891 [hep-lat].
- [35] M. Della Morte, B. Jäger, T. Rae and H. Wittig, arXiv:1208.0189 [hep-lat].